

1
2
3
4
5
6
7 **Removal of Phenol Using Sulphate Radicals Activated by Natural Zeolite Supported Cobalt**
8 **Catalysts**
9

10 Syaifullah Muhammad^{1,2}, Edy Saputra^{1,3}, Hongqi Sun¹, H. M. Ang¹, Moses O. Tadé¹, Shaobin
11 Wang^{1*}
12

13 ¹Department of Chemical Engineering and Cooperative Research Centre for Contamination
14 Assessment and Remediation of the Environment (CRC-CARE), Curtin University, GPO Box
15 U1987, Perth, WA 6845, Australia
16

17 ²Department of Chemical Engineering, Syiah Kuala University, Banda Aceh, Indonesia
18

19 ³Department of Chemical Engineering, Riau University, Pekanbaru, Indonesia
20

21 *Corresponding Author: Shaobin.wang@curtin.edu.au
22
23
24

25 **Abstract**
26

27 Two Co oxide catalysts supported on natural zeolites from Indonesia (INZ) and Australia (ANZ)
28 were prepared and used to activate peroxymonosulphate for degradation of aqueous phenol. The
29 two catalysts were characterized by several techniques such as X-ray diffraction (XRD), scanning
30 electron microscopy (SEM), energy dispersive X-ray spectroscopy (EDS), and N₂ adsorption. It was
31 found that Co/INZ and Co/ANZ are effective in activation of peroxymonosulphate to produce
32 sulphate radicals for phenol degradation. Co/INZ and Co/ANZ could remove phenol up to 100%
33 and 70%, respectively, at the conditions of 25 ppm phenol (500 mL), 0.2 g catalyst, 1 g oxone, and
34 25 °C. Several parameters such as amount of catalyst loading, phenol concentration, oxidant
35 concentration and temperature were found to be the key factors influencing phenol degradation. A
36 pseudo first order would fit to phenol degradation kinetics and the activation energies on Co/INZ
37 and Co/ANZ were obtained as 52.4 and 61.3 kJ/mol, respectively.
38
39

40 **Key words:** Heterogeneous oxidation; sulphate radical; phenol degradation; natural zeolite; Co
41 oxide
42
43
44
45
46
47

48 **1. Introduction**

49 Phenolic compounds are important organic pollutants in wastewater, which can be produced in
50 chemical, petrochemical, and pharmaceutical industries (Ahmaruzzaman, 2008, Busca, et al., 2008).
51 This type of organic contaminants can not be easily removed in primary and secondary treatment
52 processes. Therefore, it is essential to adopt a tertiary treatment such as thermal oxidation, chemical
53 oxidation, wet air oxidation, catalytic oxidation etc, which are generally known as advanced
54 oxidation processes (AOPs) (Parmeggiani and Cardona, 2012, Wang and Xu, 2012, Shukla, et al.,
55 2010). In principle, the AOPs will produce harmless compounds to the environment such as CO₂
56 and H₂O. Among the AOPs, heterogeneous catalytic oxidation usually has some advantages such as
57 operating at room temperature with normal pressure and low energy. Furthermore, heterogeneous
58 catalysts can be synthesized using cheap materials as supports such as activated carbon, silica,
59 alumina and zeolites (Saputra, et al., 2012). Among the materials, zeolites are important
60 heterogeneous catalysts used in industry. Their key properties are size and shape selectivity,
61 together with the potential for strong acidity. Zeolites also have ion exchangeable sites and highly
62 hydrothermal stability, making them widely used for many applications in separation, ion exchange
63 and adsorption. Natural zeolites are much cheaper than synthetic zeolites due to their wide
64 availability in the world (Wang and Peng, 2010). However, few investigations have been reported
65 in use of natural zeolites for AOPs (Valdes, et al., 2009).

66 Currently, most of AOPs are based on the generation of very reactive species, such as hydroxyl
67 radicals (OH•), which will oxidize many pollutants quickly and non selectively (Wang and Xu,
68 2012, Dhakshinamoorthy, et al., 2012, Wang, 2008). Recently, sulphate radicals have also been
69 proposed as alternative active oxidants due to their higher oxidation potential (Zhou, et al., 2011,
70 Ling, et al., 2010). For sulphate radical production, peroxymonosulphate (PMS, HSO₅⁻) reaction
71 with Co ions has been found to be an effective route (Anipsitakis and Dionysiou, 2003, Anipsitakis
72 and Dionysiou, 2004).

73 However, the use of Co metal ion as a catalyst to activate PMS for generation of sulphate radicals
74 raises an issue of toxicity of the cobalt ions in water, because Co is one of heavy metals which can
75 cause diseases to animals and human beings. Thus, employing Co²⁺/PMS for oxidation of aqueous
76 pollutants and minimizing the discharge of cobalt in wastewater require development of an efficient
77 heterogeneous catalytic system by incorporating cobalt ions in a substrate. In addition, it is easy to
78 recover the used catalysts after simple separation process. In the past years, several types of
79 heterogeneous cobalt catalyst including cobalt oxides (Anipsitakis, et al., 2005, Chen, et al., 2008),
80 cobalt composite (Yang, et al., 2009) and supported cobalt catalysts have been investigated (Yang,
81 et al., 2008, Hu, et al., 2011, Shukla, et al., 2010, Shukla, et al., 2010, Shukla, et al., 2011, Shukla,
82 et al., 2011, Hardjono, et al., 2011).

84 In the previous investigations, synthetic materials were employed and they are usually expensive.
85 Moreover, some of the supported catalysts did not show good activity. Natural zeolites are cheaper
86 porous aluminosilicate materials and have been used for adsorbents and catalyst supports. However,
87 no work has been reported for natural zeolite supported Co catalysts in PMS activation water
88 treatment. In this research, we investigate cobalt based catalysts supported on Indonesian natural
89 zeolite (INZ) and Australian natural zeolite (ANZ) for heterogeneous generation of sulphate
90 radicals for chemical mineralization of phenol in the solution. Several key parameters in the kinetic
91 study such as phenol concentration, catalyst loading, oxone concentration and temperature were
92 investigated.

93
94

95 **2. Materials and Methods**

96
97

97 **2.1 Synthesis of natural zeolite supported cobalt catalysts**

98
99

99 Cobalt/Indonesian-natural-zeolite (Co/INZ) and cobalt/Australian-natural-zeolite (Co/ANZ) were
100 synthesized using an impregnation method. INZ and ANZ samples were crushed in particle size of
101 60-100 μm . Cobalt nitrate ($\text{Co}(\text{NO}_3)_2 \cdot 6\text{H}_2\text{O}$, Sigma-Aldrich) was dissolved into 200 mL ultrapure
102 water. Then, INZ or ANZ was added into the solution and kept stirring for 24 h. The solid was dried
103 in an oven at 120 $^\circ\text{C}$ for 6 h. Calcination of the catalysts was conducted in a furnace at 550 $^\circ\text{C}$ for 6
104 h. For the two catalysts, Co loading was kept at 5 wt%.

105
106

105 **2.2 Characterization of catalysts**

106 The synthesized catalysts were characterized by XRD, SEM combined with EDS, and N_2
107 adsorption. Crystalline structure of the materials was analyzed by a X-ray diffractometer (Bruker
108 D8 Advance equipped with a Lynx eye detector, Bruker-AXS, Karlsruhe, Germany) operated at 40
109 kV and 30 mA. SEM (Philips XL30) with secondary and backscatter electron detectors at 15 kV
110 and 7 mm distance was used to obtain a visual image of the samples to show the texture and
111 morphology of the catalysts with magnification up to 8000 times. The catalysts were also
112 characterized by EDS (Energy Dispersive X-ray spectroscopy) to identify the structural features and
113 the mineralogy. Furthermore, nitrogen adsorption (Micromeritics Gemini 2360) was used to obtain
114 the BET surface area (S_{BET}). Prior to the analysis, the catalyst samples were degassed under vacuum
115 at 200 $^\circ\text{C}$ for 12 h.
116

117
118

118 **2.3 Kinetic study of phenol oxidation**

119
120

120 Catalytic oxidation of phenol was conducted in 500 mL phenol solutions with concentrations of 25 -
121 100 ppm. A reactor attached to a stand was dipped into a water bath with a temperature control. The
122 solution was stirred constantly at 400 rpm to maintain a homogeneous solution. A fixed amount of

123 oxidant of peroxymonosulphate (using oxone, DuPont's triple salt $2\text{KHSO}_5 \cdot \text{KHSO}_4 \cdot \text{K}_2\text{SO}_4$,
124 Aldrich) was added to the mixture until completely dissolved. Then, a fixed amount of catalysts
125 (Co/INZ or Co/ANZ) was added into the reactor for running of 3-5 h. At the fixed time interval, 0.5
126 mL of solution sample was withdrawn and filtered using a HPLC standard filter of 0.45 μm and
127 mixed with 0.5 mL methanol as a quenching reagent to stop the reaction. Phenol was then analyzed
128 on a HPLC with a UV detector at wavelength of 270 nm. The column is C18 with mobile phase of
129 70% acetonitrile and 30% ultrapure water.

130

131 **3 Results and Discussion**

132

133 **3.1 Characterization of natural zeolite supported cobalt catalysts**

134

135 XRD patterns of Co/INZ and Co/ANZ are presented in Fig.1. Co_3O_4 peaks were identified on both
136 catalysts, however, the peaks are weaker and broad on Co/INZ. This suggested that dispersion of
137 Co_3O_4 crystallites on INZ was higher and thus more active sites (Co_3O_4) were produced on Co/INZ,
138 which could enhance reaction rate. N_2 adsorption showed that the BET surface areas of INZ and
139 ANZ are 30.5 and 16.0 m^2/g , respectively, while the BET surface areas of Co/INZ and Co/ANZ are
140 17.9 and 8.1 m^2/g , respectively. In general, high surface area of a support will result in high
141 dispersion of active metal on the support.

142

143

[Insert Fig.1]

144

145

146 SEM images and EDS spectra of Co/INZ and Co/ANZ catalysts are shown in Fig. 2 and Fig. 3.
147 Both secondary electron (SE) and backscattered (BSE) detectors were adopted to observe the
148 dispersion of active cobalt on the catalyst support. From Fig. 2A and 2B, it can be seen that the BSE
149 detector produces the brighter image than the SE detector at the same observed area. This brighter
150 area refers to the presence of cobalt specks on Co/INZ particles. It also implies that cobalt was well
151 dispersed and coated on the natural zeolite support. The presence of cobalt in the catalyst was also
152 confirmed by EDS spectra (Fig. 2C).

153

[Insert Figure 2]

154

155 A similar observation was also obtained on Co/ANZ catalyst (Fig. 3). However, the particle size of
156 Co/ANZ seems to be larger than Co/INZ. BSE image also shows a good dispersion of cobalt on
157 Co/ANZ surface confirmed by EDS spectra. Thus, compared with Co/INZ, Co/ANZ presents larger
158 particle size but low Co dispersion.

159

160

[Insert Figure 3]

161

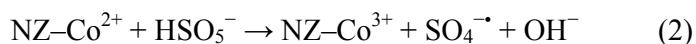
162
163
164
165
166
167
168
169
170
171
172
173
174
175
176
177
178
179
180
181
182
183
184
185
186
187
188
189
190
191
192
193
194
195
196
197
198
199
200

3.2 Phenol oxidation

Adsorption and oxidation of phenol on Co/INZ and Co/ANZ are presented in Fig. 4. In the presence of only oxone in phenol solution, no phenol degradation occurred, indicating that oxone itself could not produce sulphate radicals to induce phenol oxidation. Both Co/INZ and Co/ANZ presented low adsorption of phenol at less than 10% in 5 h. However, Co/INZ presented a slight higher phenol adsorption than Co/ANZ, which can be ascribed to higher surface area of Co/INZ.

[Insert Figure 4]

In oxidation tests, Co/INZ with the presence of PMS could degrade phenol up to 100% in 5 h. Meanwhile, Co/ANZ could reach around 70% phenol removal. Significant degradation of phenol in the systems confirms that cobalt in both catalysts could activate PMS to generate sulphate radicals ($\text{SO}_4^{\cdot-}$ and $\text{SO}_5^{\cdot-}$) for phenol decomposition in solution. XRD analyses showed that Co_3O_4 is major Co species in both catalysts, which will play the role for oxone activation. The reaction mechanism can be listed as below.



Adsorption tests showed that Co/INZ presented higher phenol adsorption than Co/ANZ. XRD also indicated that Co dispersion on Co/INZ is higher than that on Co/ANZ. SEM images show smaller particle size of the catalyst, Co/INZ. For heterogeneous oxidation, high surface adsorption of phenol and more active Co oxide on surface will promote catalytic activity. Thus, Co/INZ exhibits higher activity than Co/ANZ, achieving 100% phenol removal in less time. Some investigations using different supported Co catalysts have been reported. It was reported that Co/ZSM5 could achieve complete degradation of phenol in 6 h (Shukla, et al., 2010) and that Co/SiO₂ could make 100% phenol degradation at 350 min (Shukla, et al., 2011). Therefore, Co/INZ is better than Co/ZSM5 and Co/SiO₂.

Several variables influencing phenol degradations were also investigated. The effect of initial phenol concentration at 25, 50, 75 and 100 mg/L on phenol degradation is shown in Fig. 5. Phenol degradation efficiency decreased with increasing phenol concentration. The 100% phenol removal could be achieved at phenol concentration of 25 mg/L in 5 h by using Co/INZ catalyst. While in the same duration at phenol concentrations of 50, 75 and 100 mg/L, removal efficiency obtained are 50, 40 and 30%, respectively. For phenol degradation in Co/INZ-oxone, phenol degradation rate is dependent on the concentration of sulphate radicals. Due to the same concentrations of Co/INZ and

201 PMS, sulphate radical concentration produced in solution will be the same. Thus, high amount of
202 phenol in solution will require more time to achieve the same removal rate, thus lowering phenol
203 degradation efficiency.

204 **[Insert Figure 5]**
205

206 Phenol removal efficiency is also affected by catalyst loading in the system as shown in Fig. 6. A
207 complete removal of phenol could be reached within 5 h at 0.4 g/L Co/INZ loading. While 70% and
208 40% removals could be reached at Co/INZ loading of 0.2 and 0.1 g/L, respectively. For phenol
209 degradation, increased catalyst loading would enhance phenol adsorption and Co oxide to activate
210 PMS, resulting in high phenol degradation.

211 **[Insert Figure 6]**
212
213

214 The effect of oxone concentration on the removal efficiency of phenol is presented in Fig. 7. For
215 both catalysts, higher oxone concentration resulted in higher phenol removal. At reaction time of 3
216 h, the highest removal efficiency of phenol was obtained at 2 g/L oxone and the lowest was at 0.5
217 g/L oxone on Co/ANZ. However, phenol degradation would reach a similar level after oxone
218 loading higher than 1 g/L on Co/INZ, suggesting the optimal loading at 1 g/L.

219 **[Insert Figure 7]**
220
221

222 In addition, temperature is also a key factor influencing catalyst activity and phenol degradation.
223 Fig.8 shows the effect of temperature on phenol degradation. Higher phenol removal was obtained
224 at increased temperature. For instance, at reaction time of 3 h, removal efficiencies of phenol on
225 Co/ANZ at 25, 35, and 45 °C were 45, 75 and 100%, respectively (Fig. 8B). A similar trend is also
226 obtained on Co/INZ catalyst and the removal efficiencies increased from 80% at 25 °C to 100% at
227 35 and 45 °C.

228 **[Insert Figure 8]**
229
230

231 For variation of phenol degradation with time, a first order model as shown in equation below was
232 used to fit kinetics.
233

234
235
$$C = C_0 e^{(-k \cdot t)} \quad (3)$$

236 Where k is the first order rate constant of phenol removal, C is the concentration of phenol at
237 various time (t), C_o is the initial concentration of phenol.

238 Fig.8 also shows the curves of phenol degradation kinetics from the first order model and it is seen
239 that phenol degradation on Co/INZ and Co/ANZ catalysts could be well fitted by the model. The
240 rate constant and regression coefficients are presented in Table 1. Several heterogeneous Co
241 catalysts have been tested in PMS activation for phenol degradation. It was found that phenol
242 degradation on Co/SiO₂ (Shukla, et al., 2011) and Co/ZSM5 (Shukla, et al., 2010) presented zero
243 order kinetics while Co/AC showed the first order kinetics (Shukla, et al., 2010). Chen et al. (Chen,
244 et al., 2007) also found the pseudo first-order for decolourization of acid orange 7 (AO7) in aqueous
245 Co²⁺/oxone system.

246

247

[Insert Table 1]

248

249 Fig.9 shows the relationship between rate constants (k) and temperatures by the Arrhenius
250 correlation. It can be seen that a good relationship for both catalysts was achieved and activation
251 energies for phenol degradation on Co/ANZ and Co/INZ were obtained at 52.4 and 61.3 kJ/mol,
252 respectively.

253

[Insert Figure 9]

254

255

256 **4 Conclusions**

257

258 Co/INZ and Co/ANZ are effective catalysts for generating sulphate radicals in the presence of PMS
259 to degrade phenol. Co/INZ has better activity in removing phenol than Co/ANZ. Phenol removal is
260 a combination of oxidation and adsorption processes. The concentration of phenol, catalyst loading,
261 concentration of oxone, and temperature are key parameters affecting the reaction rate in phenol
262 degradation. Kinetic studies show that phenol oxidation on the Co/INZ and Co/ANZ follows the
263 first order reaction with the activation energies of 52.4 and 61.3 kJ/mol, respectively.

264

265 **Acknowledgements**

266

267 We thank DIKTI sponsor, National Education Department of Indonesia Government, for providing
268 a scholarship to SM and ES for their Ph.D study.

269

270

271 **References**

272

273 Ahmaruzzaman, M. (2008). Adsorption of phenolic compounds on low-cost adsorbents: A review,
274 *Advances in Colloid and Interface Science*, 143, 48-67.

- 275 Anipsitakis, G.P., Dionysiou, D.D. (2003). Degradation of organic contaminants in water with
276 sulfate radicals generated by the conjunction of peroxymonosulfate with cobalt, *Environ Sci*
277 *Technol*, 37, 4790-4797.
- 278 Anipsitakis, G.P., Dionysiou, D.D. (2004). Radical generation by the interaction of transition metals
279 with common oxidants, *Environ Sci Technol*, 38, 3705-3712.
- 280 Anipsitakis, G.P., Stathatos, E., Dionysiou, D.D. (2005). Heterogeneous activation of oxone using
281 Co_3O_4 , *J Phys Chem B*, 109, 13052-13055.
- 282 Busca, G., Berardinelli, S., Resini, C., Arrighi, L. (2008). Technologies for the removal of phenol
283 from fluid streams: A short review of recent developments, *J Hazard Mater*, 160, 265-288.
- 284 Chen, X.Y., Chen, J.W., Qiao, X.L., Wang, D.G., Cai, X.Y. (2008). Performance of nano-
285 Co_3O_4 /peroxymonosulfate system: Kinetics and mechanism study using Acid Orange 7 as a
286 model compound, *Appl Catal B-Environ*, 80, 116-121.
- 287 Chen, X., Qiao, X., Wang, D., Lin, J., Chen, J. (2007). Kinetics of oxidative decolorization and
288 mineralization of Acid Orange 7 by dark and photoassisted Co^{2+} -catalyzed peroxymono
289 sulfate system, *Chemosphere*, 67, 802-808.
- 290 Dhakshinamoorthy, A., Navalon, S., Alvaro, M., Garcia, H. (2012). Metal Nanoparticles as
291 Heterogeneous Fenton Catalysts, *Chemosphere*, 5, 46-64.
- 292 Hardjono, Y., Sun, H.Q., Tian, H.Y., Buckley, C.E., Wang, S.B. (2011). Synthesis of Co oxide
293 doped carbon aerogel catalyst and catalytic performance in heterogeneous oxidation of phenol
294 in water, *Chem Eng J*, 174, 376-382.
- 295 Hu, L., Yang, X., Dang, S. (2011). An easily recyclable Co/SBA-15 catalyst: Heterogeneous
296 activation of peroxymonosulfate for the degradation of phenol in water, *Appl Catal B-*
297 *Environ*, 102, 19-26.
- 298 Ling, S.K., Wang, S.B., Peng, Y.L. (2010). Oxidative degradation of dyes in water using $\text{Co}^{2+}/\text{H}_2\text{O}_2$
299 and Co^{2+} /peroxymonosulfate, *J Hazard Mater*, 178, 385-389.
- 300 Parmeggiani, C., Cardona, F. (2012). Transition metal based catalysts in the aerobic oxidation of
301 alcohols, *Green Chemistry*, 14, 547-564.
- 302 Saputra, E., Muhammad, S., Sun, H., Ang, H.M., Tade, M.O., Wang, S. (2012). Red mud and fly
303 ash supported Co catalysts for phenol oxidation, *Catal Today*, DOI:
304 10.1016/j.cattod.2011.10.025.
- 305 Shukla, P., Fatimah, I., Wang, S.B., Ang, H.M., Tade, M.O. (2010). Photocatalytic generation of
306 sulphate and hydroxyl radicals using zinc oxide under low-power UV to oxidise phenolic
307 contaminants in wastewater, *Catal Today*, 157, 410-414.
- 308 Shukla, P., Sun, H.Q., Wang, S.B., Ang, H.M., Tade, M.O. (2011). Co-SBA-15 for heterogeneous
309 oxidation of phenol with sulfate radical for wastewater treatment, *Catal Today*, 175, 380-385.
- 310 Shukla, P., Sun, H.Q., Wang, S.B., Ang, H.M., Tade, M.O. (2011). Nanosized $\text{Co}_3\text{O}_4/\text{SiO}_2$ for
311 heterogeneous oxidation of phenolic contaminants in waste water, *Sep Purif Technol*, 77, 230-
312 236.
- 313 Shukla, P., Wang, S.B., Singh, K., Ang, H.M., Tade, M.O. (2010). Cobalt exchanged zeolites for
314 heterogeneous catalytic oxidation of phenol in the presence of peroxymonosulphate, *Appl*
315 *Catal B-Environ*, 99, 163-169.
- 316 Shukla, P.R., Wang, S.B., Sun, H.Q., Ang, H.M., Tade, M. (2010). Activated carbon supported
317 cobalt catalysts for advanced oxidation of organic contaminants in aqueous solution, *Appl*
318 *Catal B-Environ*, 100, 529-534.
- 319 Valdes, H., Farfan, V.J., Manoli, J.A., Zaror, C.A. (2009). Catalytic ozone aqueous decomposition
320 promoted by natural zeolite and volcanic sand, *J Hazard Mater*, 165, 915-922.
- 321 Wang, J.L., Xu, L.J. (2012). Advanced Oxidation Processes for Wastewater Treatment: Formation
322 of Hydroxyl Radical and Application, *Critical Reviews in Environmental Science and*
323 *Technology*, 42, 251-325.
- 324 Wang, S. (2008). A Comparative study of Fenton and Fenton-like reaction kinetics in
325 decolourisation of wastewater, *Dyes Pigments*, 76, 714-720.

326 Wang, S.B., Peng, Y.L. (2010). Natural zeolites as effective adsorbents in water and wastewater
327 treatment, *Chem Eng J*, 156, 11-24.

328 Yang, Q., Choi, H., Chen, Y., Dionysiou, D.D. (2008). Heterogeneous activation of
329 peroxymonosulfate by supported cobalt catalysts for the degradation of 2,4-dichlorophenol in
330 water: The effect of support, cobalt precursor, and UV radiation, *Appl Catal B-Environ*, 77,
331 300-307.

332 Yang, Q., Choi, H., Al-Abed, S.R., Dionysiou, D.D. (2009). Iron-cobalt mixed oxide nanocatalysts:
333 Heterogeneous peroxymonosulfate activation, cobalt leaching, and ferromagnetic properties
334 for environmental applications, *Appl Catal B-Environ*, 88, 462-469.

335 Zhou, G.L., Sun, H.Q., Wang, S.B., Ang, H.M., Tade, M.O. (2011). Titanate supported cobalt
336 catalysts for photochemical oxidation of phenol under visible light irradiations, *Sep Purif
337 Technol*, 80, 626-634.

338

339 **List of Tables**

340

341 Table 1 Rate constants at different temperatures for Co/INZ and CCo/ANZ.

342

343

344

345

346

347

348

349

Table 1 Rate constants at different temperatures for Co/INZ and CCo/ANZ.

Catalyst	Temperature (°C)	Rate constant (min ⁻¹)	R ²
Co/INZ	25	7.08 x10 ⁻³	0.972
	35	0.0116	0.952
	45	0.0269	0.989
Co/ANZ	25	3.19 x10 ⁻³	0.991
	35	6.42 x10 ⁻³	0.963
	45	0.0151	0.985

350

351

352

353

354

355

356

357

358

359

360

361

362

363

364

365

366

367

368

369

370

371

372

373

374

375

376

377

378

379
380
381
382
383
384
385
386
387
388
389
390
391
392
393
394
395
396
397
398
399
400
401
402
403
404
405
406
407
408
409
410
411
412
413
414
415
416
417
418
419
420
421
422
423
424
425
426
427
428
429
430

List of Figures

Figure 1 XRD patterns of Co/ANZ and Co/INZ.

Figure 2. SEM images and EDS spectra of Co/INZ, (A) SE Detector, (B) BSE Detector, (C) EDS spectrum.

Figure 3. SEM images and EDS spectra of Co/ANZ, (A) SE Detector, (B) BSE Detector, (C) EDS spectrum.

Figure 4. Phenol reduction with time in adsorption and catalytic oxidation. Reaction condition: 0.4 g/L catalyst, 2 g/L oxone, 25 ppm phenol, 25°C and stirring speed of 400 rpm.

Figure 5. Effect of phenol concentration on phenol degradation using Co/INZ catalyst. Reaction condition: 0.4 g/L catalyst, 2 g/L oxone, 25°C and stirring speed of 400 rpm.

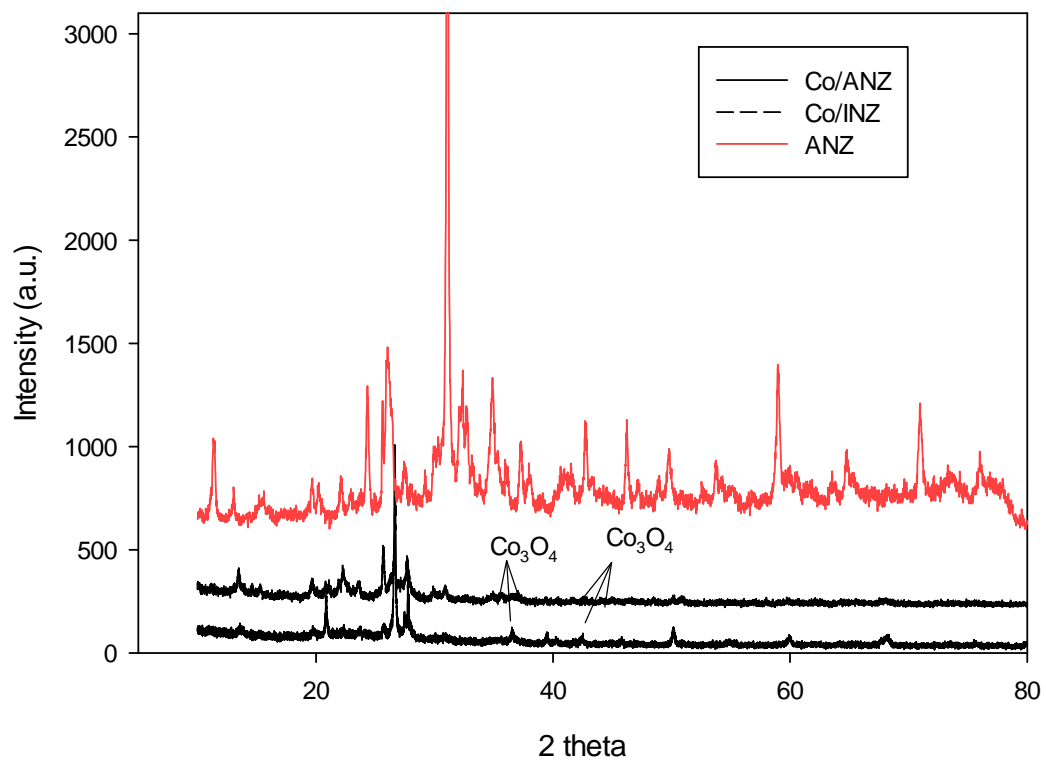
Figure 6. Effect of catalyst loading on phenol degradation using Co/INZ catalyst. Reaction condition: 2 g/L oxone, 25 ppm phenol, 25°C and stirring speed of 400 rpm.

Figure 7. Effect of oxone concentration in phenol reduction using Co/INZ catalyst. Reaction condition : 0.4 g/L catalyst, 25 ppm phenol solution, 25°C and stirring speed of 400 rpm.

Figure 8. Effect of temperature in phenol reduction, (A) Co/INZ catalyst, (B) Co/ANZ catalyst. Reaction condition : 0.4 g/L catalyst, 2 g/L oxone, 25 ppm phenol, and stirring speed of 400 rpm.

Figure 9. Arrhenius plots of phenol degradation on Co/ANZ and Co/INZ.

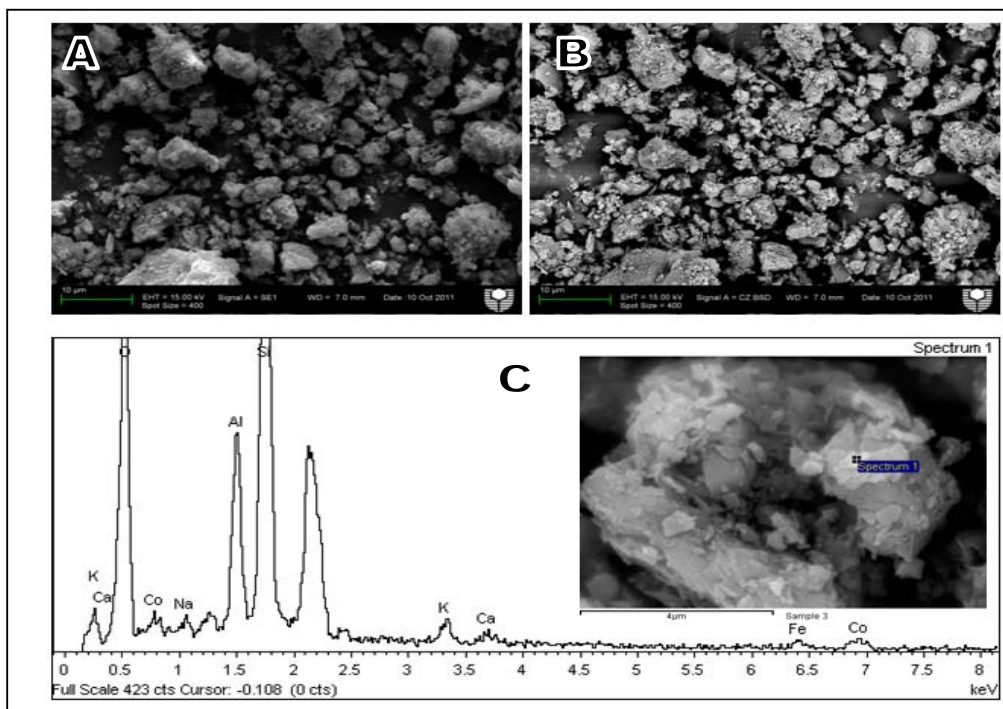
431
432
433
434
435
436



437
438
439
440
441
442
443
444
445
446
447
448
449
450
451
452
453
454
455
456
457

Fig.1 XRD patterns of Co/ANZ and Co/INZ.

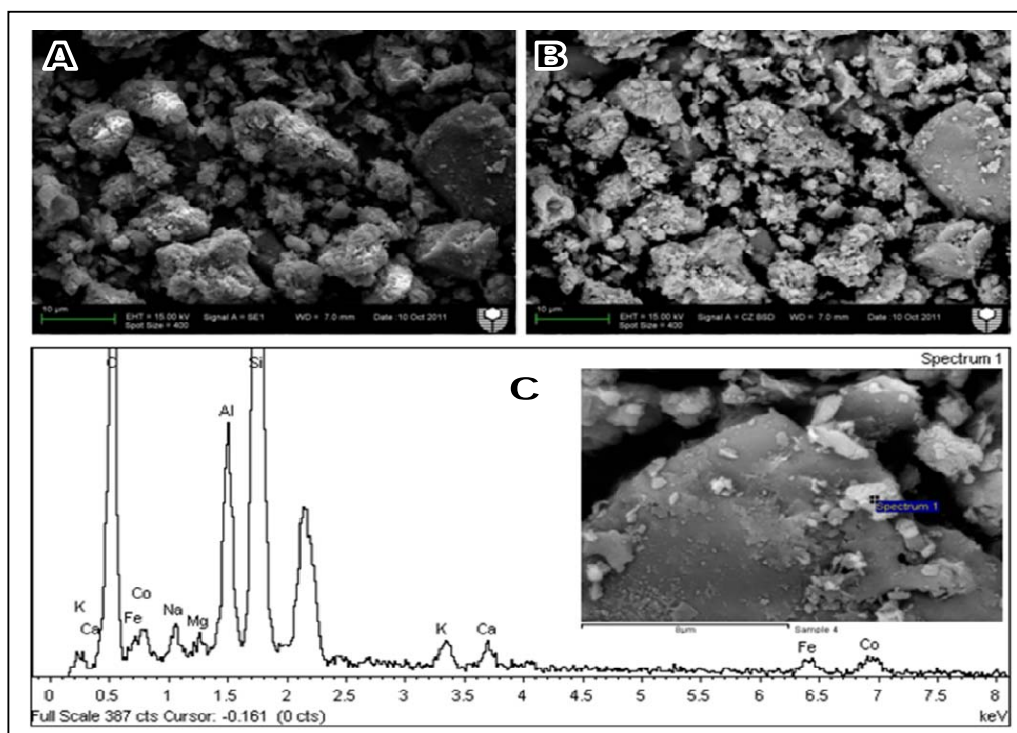
458
459
460
461
462
463
464
465
466
467
468



469
470
471
472
473
474
475
476
477
478
479
480
481
482
483
484
485
486
487
488
489
490

Figure 2. SEM images and EDS spectra of Co/INZ, (A) SE Detector, (B) BSE Detector, (C) EDS spectra with inset of spectrum image source

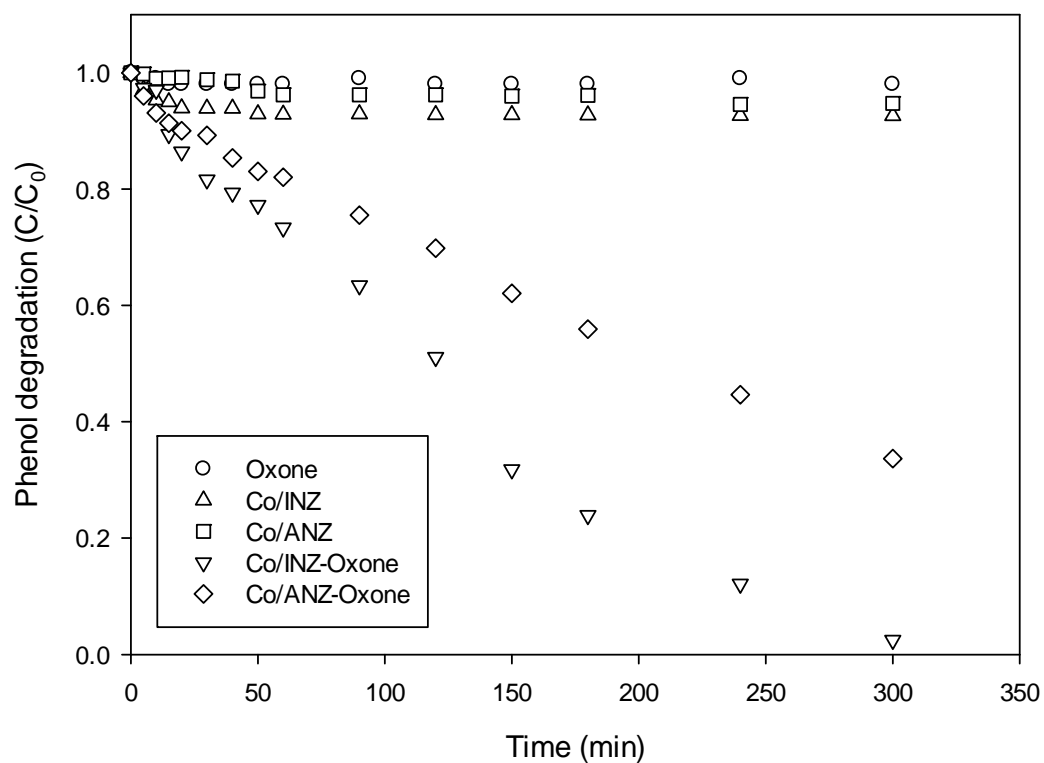
491
492
493
494
495
496
497
498
499
500
501



502
503
504
505
506
507
508
509
510
511
512
513
514
515
516
517
518
519
520
521
522

Figure 3. SEM images and EDS spectra of Co/ANZ, (A) SE Detector, (B) BSE Detector, (C) EDS spectra with inset of spectrum image source

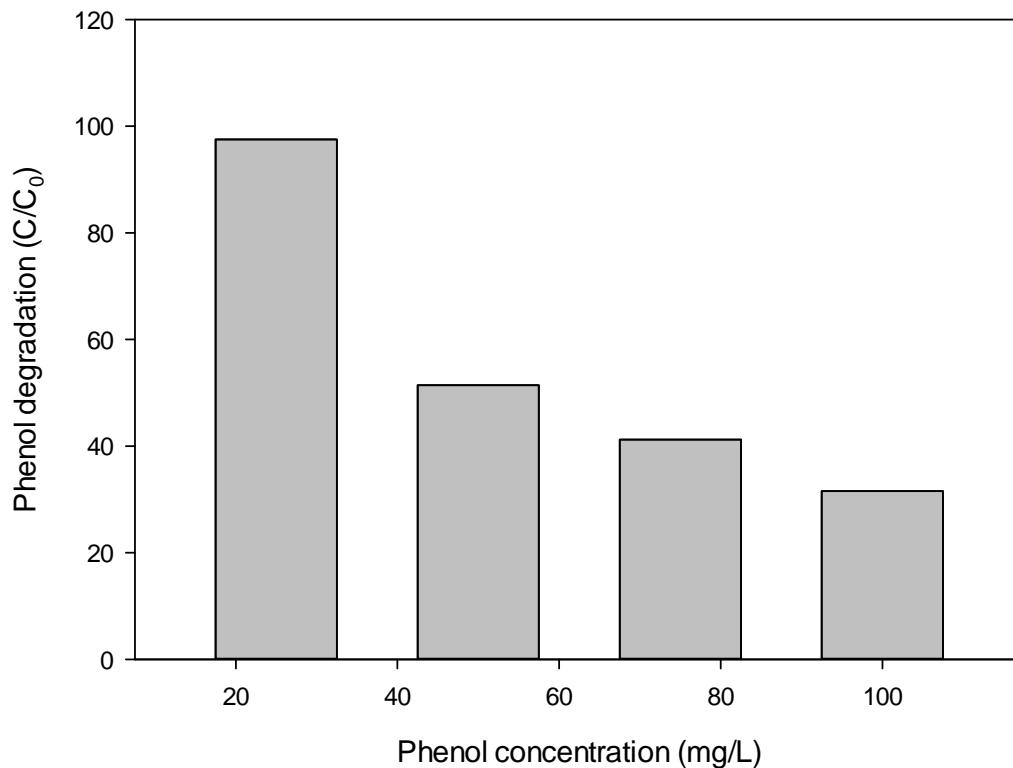
523
524
525
526
527
528
529
530
531
532
533



534
535
536
537
538
539
540
541
542
543
544
545
546
547
548
549

Figure 4. Phenol reduction with time in adsorption and catalytic oxidation. Reaction condition: 0.4 g/L catalyst, 2 g/L oxone, 25 ppm phenol, 25°C and stirring speed of 400 rpm.

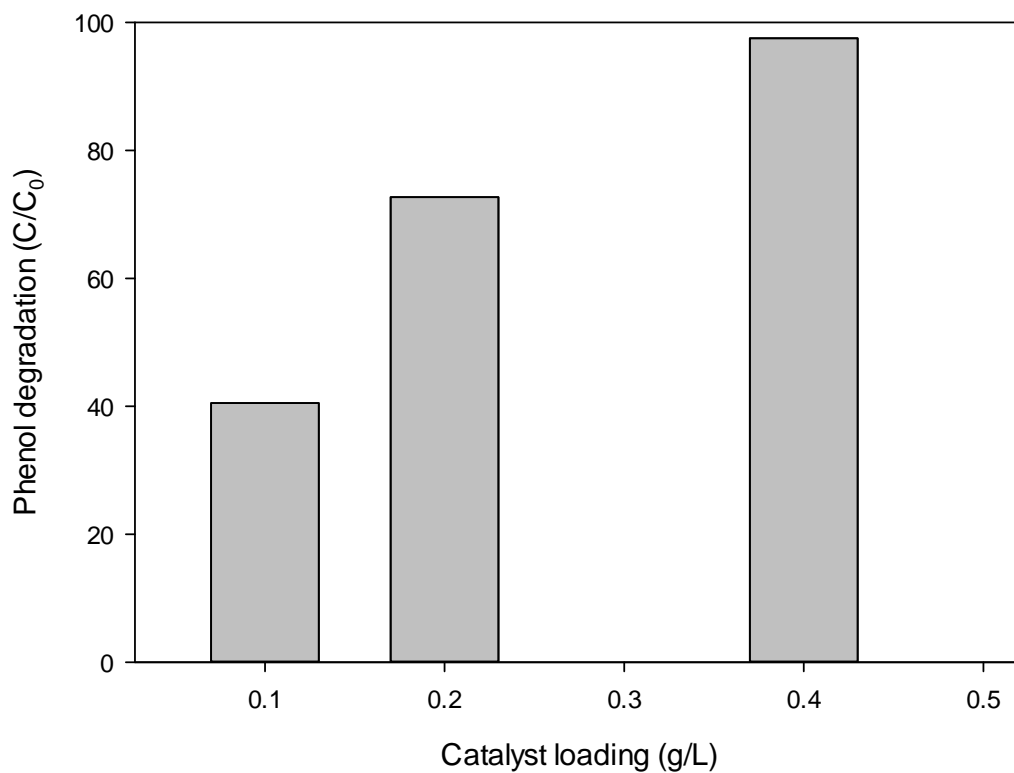
550
551
552
553



554
555
556
557
558
559
560
561
562
563
564
565
566
567
568
569
570
571
572
573
574
575
576
577

Figure 5. Effect of phenol concentration on phenol degradation using Co/INZ catalyst. Reaction condition: 0.4 g/L catalyst, 2 g/L oxone, 25°C and stirring speed of 400 rpm.

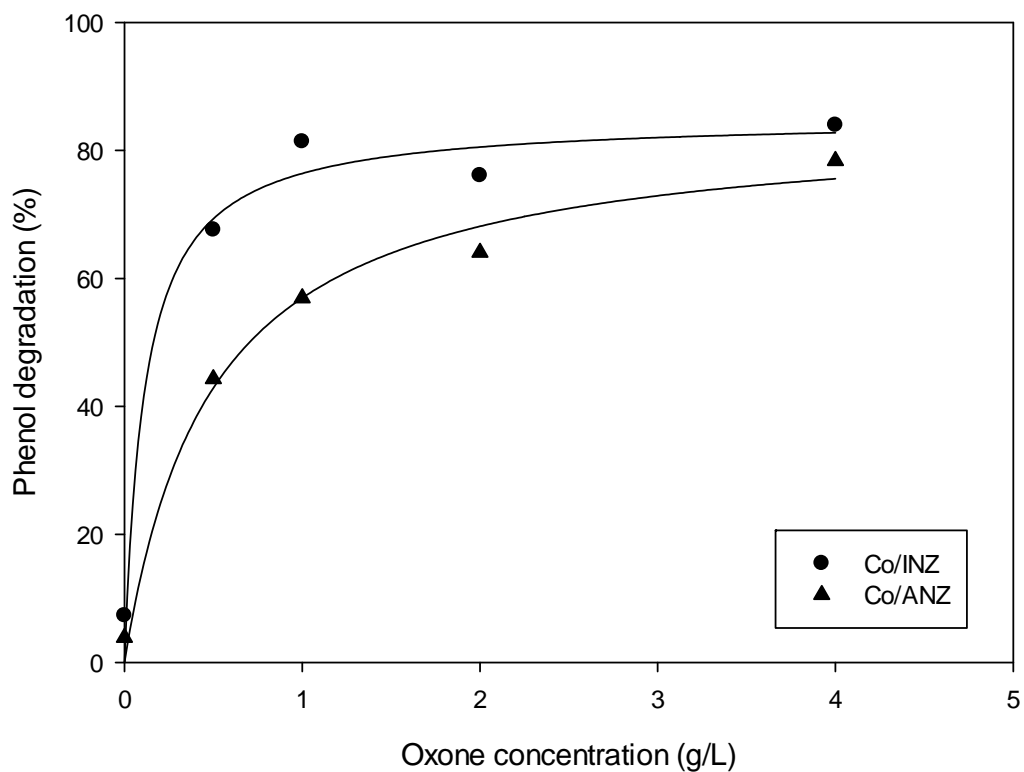
578
579
580
581
582
583
584



585
586
587
588
589
590
591
592
593
594
595
596
597
598
599
600
601
602
603
604
605

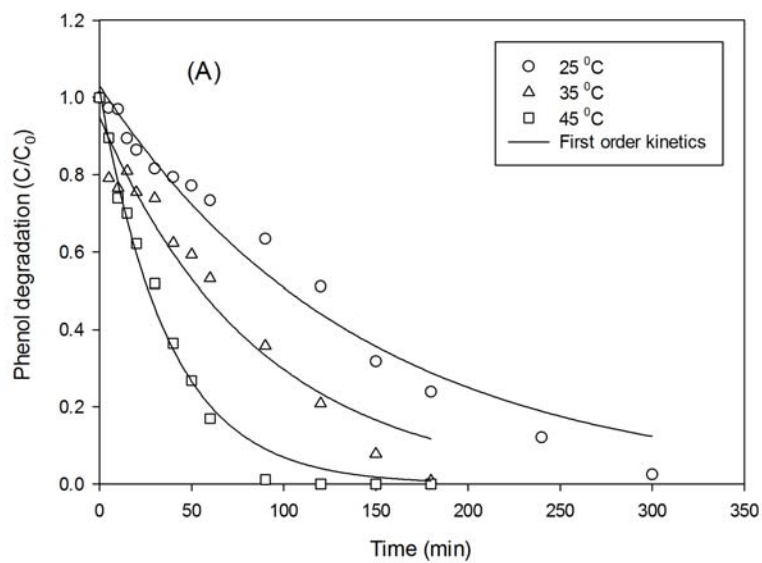
Figure 6. Effect of catalyst loading on phenol degradation using Co/INZ catalyst. Reaction condition: 2 g/L oxone, 25 ppm phenol, 25°C and stirring speed of 400 rpm.

606
607
608
609
610
611

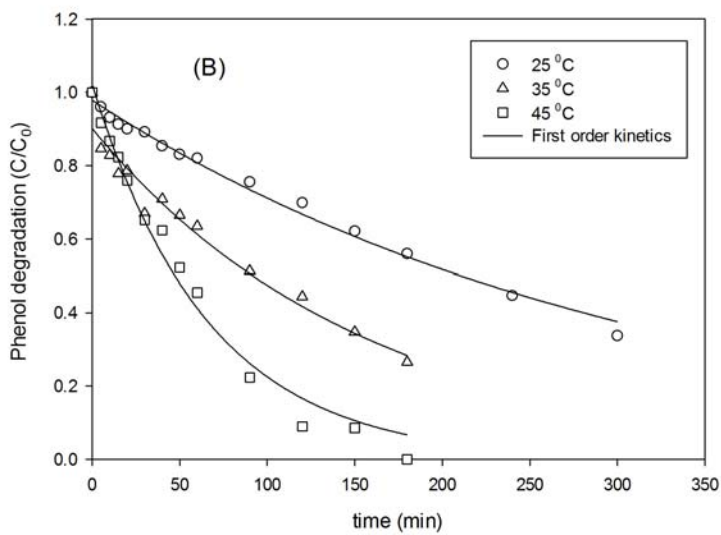


612
613
614
615
616
617
618
619
620

Figure 7. Effect of oxone concentration in phenol reduction using Co/INZ catalyst. Reaction condition : 0.4 g/L catalyst, 25 ppm phenol solution, 25°C and stirring speed of 400 rpm.



621



622

623 Figure 8. Effect of temperature in phenol reduction, (A) Co/INZ catalyst, (B) Co/ANZ catalyst.

624 Reaction condition : 0.4 g/L catalyst, 2 g/L oxone, 25 ppm phenol, and stirring speed of 400 rpm.

625

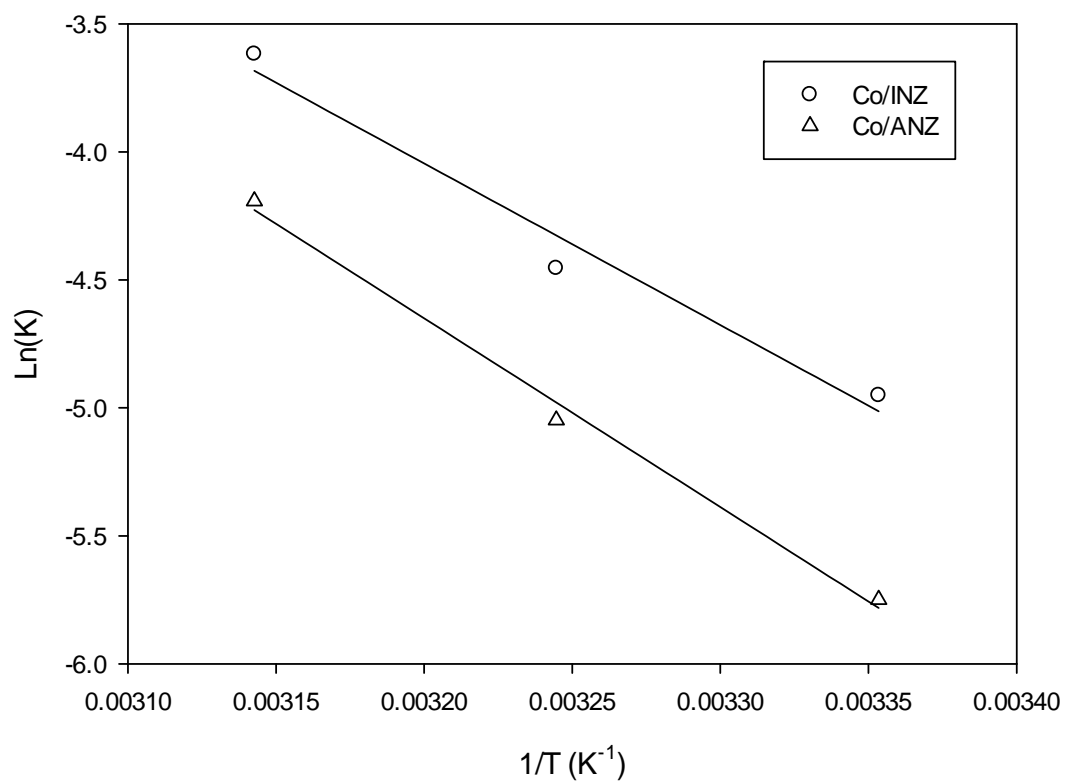
626

627

628

629

630
631
632
633
634
635
636
637
638
639



640
641
642
643
644
645

Figure 9. Arrhenius plots of phenol degradation on Co/ANZ and Co/INZ.